

Thiophene-Inserted Aryl–Dicyanovinyl Compounds: The Second Generation of Fluorescent Molecular Rotors with Significantly Redshifted Emission and Large Stokes Shift

Jingyin Shao,^[a] Shaomin Ji,^[a] Xiaolian Li,^[a] Jianzhang Zhao,^{*[a]} Fuke Zhou,^[a] and Huimin Guo^{*[a]}

Keywords: Cyanides / Fluorescence / Molecular devices / Viscosity / Density functional calculations

Fluorescent molecular rotors can be used as molecular sensors for the viscosity of a microenvironment. However, these molecular rotors are limited to 9-(dicyanovinyl)julolidine (DCVJ) and a few derivatives. Furthermore, these traditional rotors show short absorption/emission wavelengths and small Stokes shifts. To address these drawbacks, we have developed a small library of new molecular rotors for viscosity sensing, prepared by incorporating a thiophene unit into the conventional fluorescent molecular rotors with the aim of accessing molecular rotors with redshifted excitation/emission

wavelengths and larger Stokes shifts compared with the known rotors. The new rotors show substantially improved photophysical properties. For example, rotor 4 shows absorption/emission wavelengths of 559/697 nm, respectively, and a very large Stokes shift of 138 nm compared with the absorption/emission wavelengths (465/503 nm) and very small Stokes shift (38 nm) of the traditional fluorescent molecular rotor DCVJ. The photophysical properties of the rotors were rationalized by DFT calculations.

Introduction

Recently, aryl–dicyanovinyl fluorescent molecular rotors have attracted considerable attention due to their ability as fluorescent viscosity sensors (**1** and **2**, Scheme 1).^[1–11] These rotors emit weakly in fluid solution (low viscosity) due to the free rotation of the C–C/C=C bonds in the excited state, which serves as an efficient drain pipe for the photoexcited molecules. In a viscous environment, however, the intramolecular rotation is restricted, and thus the emission is greatly intensified.^[1] Well-known molecular rotors are 1-(dicyanovinyl)-4-(dimethylamino)benzene (**1**) and 9-(dicyanovinyl)julolidine (**2**, DCVJ; Scheme 1).^[1] DCVJ and a few other rotors, based on different mechanisms,^[12–14] have been used to measure the viscosity or shear stress of a microenvironment,^[1] reaction medium,^[15] or intracellular plasma.^[16,17]

However, the conventional aryl–dicyanovinyl molecular rotors for viscosity sensing [for example, DCVJ (**2**)] suffer from fundamental photophysical drawbacks, such as short absorption/emission wavelengths (465/503 nm, respectively)

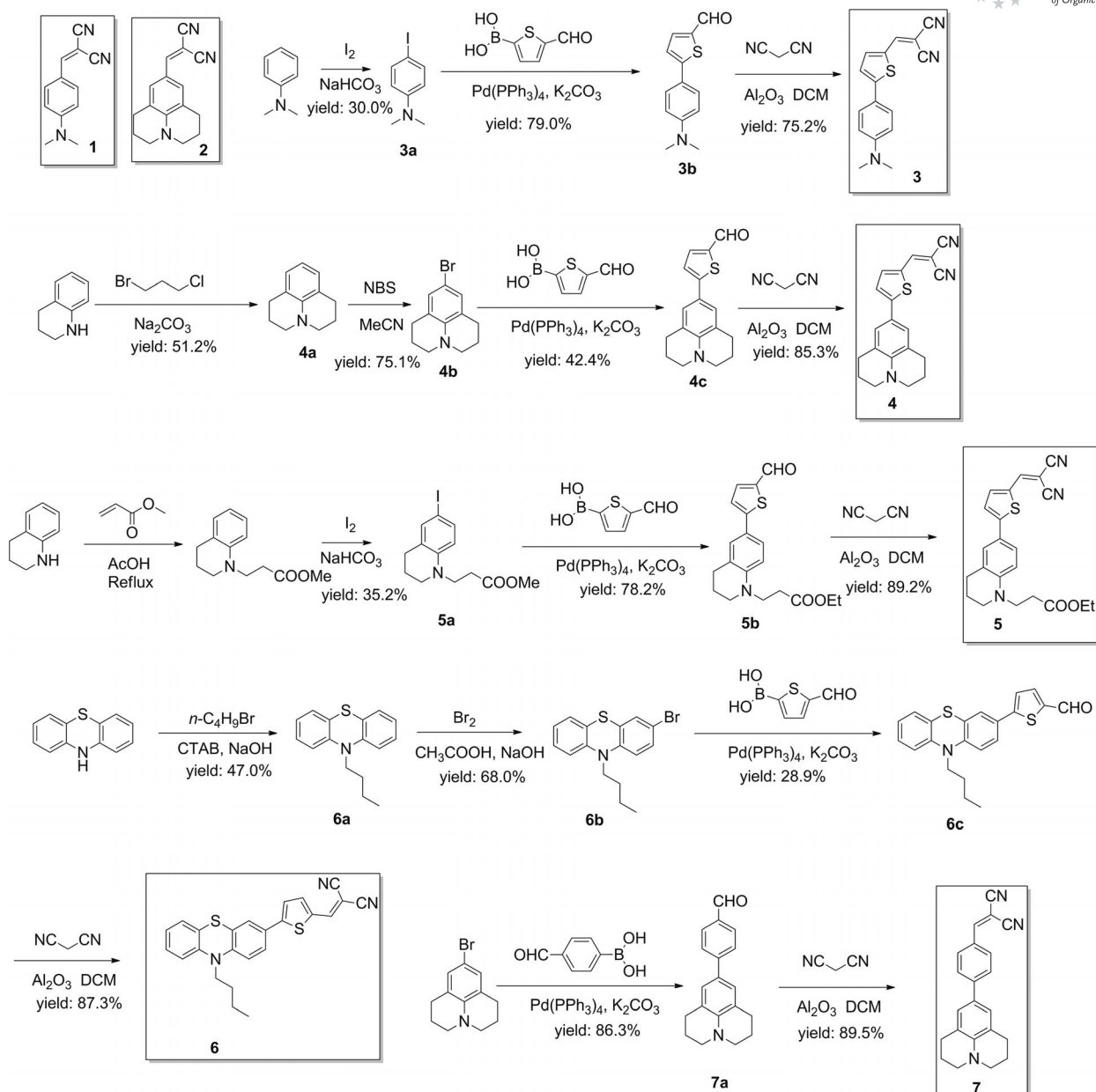
and a small Stokes shift (38 nm).^[1] A short emission wavelength makes it difficult for these sensors to be used for *in vivo* analysis due to the significant auto-fluorescence of the biological samples by excitation with UV/blue light, whereas the small Stokes shift is detrimental to the fluorescence signal, because the optical filter, which removes the excitation light from the collected emission signal, also blocks parts of the emission (due to significant overlap of the excitation and emission spectra of dyes with a small Stokes shift).^[11] To our surprise, however, there have been no reports so far on the tailoring of the structures of the aryl–dicyanovinyl molecular rotors (for example, **2**) to tackle the aforementioned photophysical drawbacks.

Recently, a BODIPY-based molecular rotor was used for *in vivo* fluorescent lifetime imaging of viscosity, but it still suffers from short absorption/emission wavelengths and an especially small Stokes shift.^[14] Porphyrin-based rotors have been reported, but the rotors are synthetically demanding.^[12,16] Therefore, simple rotors with redshifted excitation/emission and a large Stokes shift are highly desired as alternatives to DCVJ for molecular viscosity sensing.

We have been interested in the photophysics of luminophores for a while.^[18–20] Usually, the excitation/emission wavelengths of a fluorophore can be redshifted by extension of the π conjugation.^[11,18,19] A small Stokes shift usually arises from the rigidity of the fluorophore, and thus the vibration relaxation from the Franck–Condon excited state to the vibrationally relaxed S₁ state is not significant.^[11]

[a] State Key Laboratory of Fine Chemicals, School of Chemical Engineering, Dalian University of Technology, Dalian 116024, P. R. China
Fax: +86-411-8498-6236
E-mail: zhaojzh@dlut.edu.cn
guohm@dlut.edu.cn

Supporting information for this article is available on the WWW under <http://dx.doi.org/10.1002/ejoc.201100891>.



Scheme 1. Synthesis of thiophene-containing fluorescent molecular rotors **3–6** and control compound **7**. The known rotors **1** and DCVJ (**2**) are also shown.

Thus, a large Stokes shift can be achieved by increasing the flexibility of the fluorophore skeleton. On this basis, we inserted a thiophene moiety into the aryl–dicyanovinyl rotors to extend the π conjugation of the molecules and at the same time increase their vibrational flexibility (Scheme 1) and thus redshift the excitation/emission wavelengths and, more importantly, increase the Stokes shift of the molecular rotors.

Herein we demonstrate the greatly improved photophysical properties, that is, the redshifted excitation/emission wavelengths and increased Stokes shifts, observed for the new molecular rotors **3–6** (Scheme 1). Furthermore, we prove that a rotor with an attached carboxylic acid can be readily constructed by our strategy (for example, rotor **5**,

which can be used to label biomolecules).^[8] We also demonstrate that our approach can be extended to other fluorophores (rotors **6**). The specific effect of thiophene insertion on the photophysical properties of the rotors is demonstrated by a control rotor with a phenylene linker (**7**).

Results and Discussion

Design of the Fluorescent Molecular Rotors

The main goal of our study was to prepare molecular rotors with redshifted absorption/emission wavelengths and Stokes shifts larger than those of the known molecular probes **1** and **2** (Scheme 1). In principle, this goal can be

achieved by extension of the π -conjugated framework of the chromophore of the rotors. Recently, we showed that the acetylene bond can be used to extend the absorption/emission wavelengths of the rotors.^[21] However, we found that the sensitivity of the resulting rotors to viscosity was reduced. Thus, we set out to explore another strategy to improve the photophysical properties of the rotors. The thiophene moiety is extensively used in materials chemistry (for example, in sensitizers in dye-sensitized solar cells),^[22,23] very often as a π -conjugation linker. Recently, we proved that the thiophene moiety can be used as an efficient π -conjugation linker in fluorescence boronic acid sensors to move the absorption/emission to the red end of the spectrum.^[24] Thus, in this work we devised new molecular rotors containing thiophene (Scheme 1). Insertion of the thiophene moiety into the traditional rotors (compounds **1** and **2**) leads to new rotors **3** and **4**. Rotor **5** was designed with a carboxylic group attached, and thus this rotor can be used for labeling.^[6,25,26] Furthermore, we used a different chromophore to construct the molecular rotors, that is, the phenothiazine chromophore, which is a known electron-donating moiety.^[27] Rotor **7** was prepared as a control compound to prove that the thiophene moiety can be used as an efficient π -conjugation linker, but not the phenyl moiety.

UV/Vis Absorption and Fluorescence Spectra of the New Rotors

The UV/Vis absorption and fluorescence emission of the new rotors were studied and compared with those of the traditional rotors **1** and **2** (Scheme 1). Redshifted absorption and emission wavelengths were observed for the new rotors. For example, **4** shows absorption/emission at 559/697 nm, respectively (Figure 1, Table 1), which are greatly redshifted compared with DCVJ (**2**; $\lambda_{\text{ab}}/\lambda_{\text{em}} = 465/503$ nm, respectively).^[1] The emission of **4** is redshifted by around 194 nm compared to that of DCVJ. The broad excitation/emission bands are probably due to the intramolecular charge-transfer nature of **4**. In particular, a large Stokes shift of 138 nm is observed for **4**, which compares with the

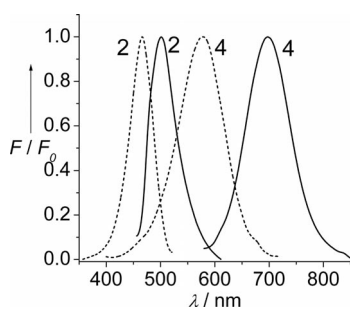


Figure 1. Normalized fluorescence excitation and emission spectra of DCVJ (**2**; $\lambda_{\text{ex}} = 465$ nm, $\lambda_{\text{em}} = 503$ nm) and rotor **4** ($\lambda_{\text{ex}} = 559$ nm, $\lambda_{\text{em}} = 697$ nm; $c = 1.0 \times 10^{-6}$ mol/L in ethylene glycol, 20 °C).

small Stokes shift of 38 nm for DCVJ (**2**).^[1] These greatly improved photophysical properties of **4** are beneficial for in vivo molecular viscosity sensing. Similar results were found for **3** ($\lambda_{\text{ab}}/\lambda_{\text{em}} = 513/661$ nm, respectively). A Stokes shift of 148 nm was observed for **3** (see the Supporting Information).

Table 1. Photophysical parameters of rotors **1**–**7** [the data of reported molecular rotors **1** and DCVJ (**2**) are included for comparison].

Rotor	Solvent	$\lambda_{\text{abs}}^{\text{[a]}}$ [nm]	$\lambda_{\text{em}}^{\text{[b]}}$ [nm]	Stokes shifts [nm]	$\tau^{\text{[c]}}$ [ns]	$\Phi^{\text{[d]}}$
1	DCM	433	474	41	2.44	0.0059
	ethylene glycol	441	482	41	0.16	0.0078
	glycerol	443	485	42	0.22	0.0951
2	DCM	458	491	33	0.55	0.0058
	ethylene glycol	465	503	38	0.18	0.0082
3	glycerol	472	505	33	0.28	0.0755
	DCM	508	620	102	0.95	0.0804
4	ethylene glycol	513	661	148	0.39	0.0235
	glycerol	522	655	133	1.24	0.0695
	DCM	553	664	111	2.11	0.1229
5	ethylene glycol	559	697	138	0.71	0.0066
	glycerol	572	689	117	0.89	0.0279
	DCM	524	631	107	1.52	0.1091
6	ethylene glycol	530	670	140	0.54	0.0280
	glycerol	536	664	128	1.26	0.0656
	DCM	488	734	246	0.36	0.0014
7	ethylene glycol	485	669	184	– ^[e]	0.0001
	glycerol	497	652	155	1.29	0.0062
	DCM	502	683	181	0.17	0.0037
7	ethylene glycol	501	603	102	0.30	0.0007
	glycerol	512	580	68	1.41	0.0077

[a] UV/Vis absorption maximum. [b] Emission maximum. [c] Fluorescence lifetime. [d] Fluorescence quantum yield, with quinine sulfate as standard ($\Phi = 54.7\%$ in 0.05 M H_2SO_4). [e] Not determined due to the weak emission.

Viscosity Dependency of the Fluorescence Emission of the Rotors

First we investigated the emission spectra of rotor **4** in methanol, ethylene glycol, and glycerol to study the effect of solvent viscosity on the emission intensity of rotor **4** (Figure 2). The emission of rotor **4** in methanol is weak,

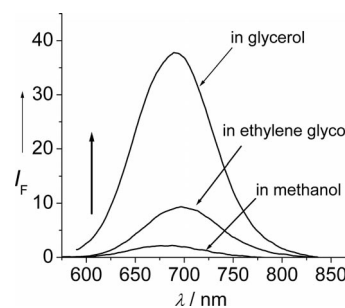


Figure 2. Emission spectra of **4** in methanol, ethylene glycol, and glycerol. The emission intensity at 690 nm in glycerol is 17.5-fold that in methanol ($c = 1.0 \times 10^{-5}$ mol/L, 20 °C).

but can be greatly enhanced in solvents with much higher viscosity, such as ethylene glycol and glycerol. These results indicate that the fluorescence intensity of rotor **4** can be enhanced by increasing the viscosity of the solvent (micro-environment).

The sensitivity of **4** to viscosity was studied quantitatively (Figure 3a). The emission intensity of **4** at 697 nm was increased by around 4.5-fold by increasing the viscosity of the solvent (13.5–945 cP), which is a comparable increase to that of DCVJ (ca. 4.0-fold, 49–631 cP).^[1] Notably, the emission enhancement of **4** by increasing the viscosity from 0.59 to 945 cP from MeOH to glycol, is around 17-fold (see the Supporting Information). The emission intensity of the rotors and the viscosity can be correlated by the Förster–Hoffmann equation [Equation (1)] in which η is the viscosity, I is the emission intensity, C is a constant, and x is the sensitivity of the rotor to viscosity.

$$\log I = C + x \log \eta \quad (1)$$

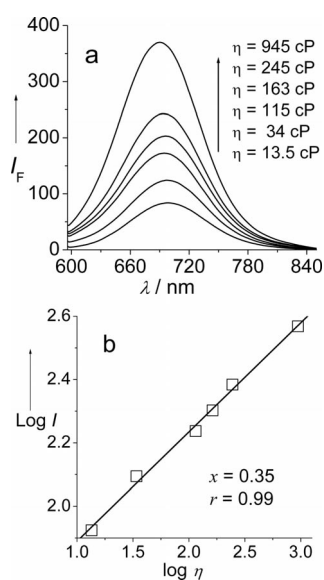


Figure 3. Fluorescence spectra of **4**. (a) Emission of **4** in ethylene glycol/glycerol mixtures of different viscosity. (b) Fitting of the data to the Förster–Hoffmann equation ($c = 1.0 \times 10^{-6}$ mol/L, 20 °C).

A perfect linear fitting was observed with a value of x of 0.35 for **4** (Figure 3b) and a large value of x (0.468) for rotor **4** in the low-viscosity range (0.59–13.5 cP, see the Supporting Information). These values are comparable to the x value of DCVJ (0.59). Interestingly, the emissions of the new rotors are sensitive to the polarity of the solvent, which is valuable for dual-functional in vivo molecular sensing of polarity and viscosity.^[1,2]

Our thiophene insertion approach can be readily extended to more functionalized derivatives such as **5** (Scheme 1). Compound **5** shows similar absorption/emis-

sion wavelengths (530/670 nm), large Stokes shift (140 nm) and x value (0.305; see the Supporting Information). With the carboxylic ester moiety, **5** can be used for labeling bio-molecules.^[6,25,26]

The molecular structures of the thiophene-containing molecular rotors are characterized as D– π –A, and thus we expected that the fluorescence emissions of these molecular rotors may be sensitive to solvent polarity. Note that this is not necessarily the case, because the traditional molecular rotors, such as rotors **1** and **2**, do not show polarity-dependent emission. We found that the UV/Vis absorption and fluorescence emission of rotor **4** are sensitive to solvent polarity (Figure 4). The sensitivity was quantitatively evaluated by the Lippert–Matage relationship and the correlation between the Stokes shift and $E_T(30)$ values (Figure 5).^[28] Similar results were found for the other molecular rotors described herein (see the Supporting Information). The traditional rotors do not show solvent-polarity-dependent emission wavelengths. Thus, we propose that the changes in the dipole moments of the new rotors upon photoexcitation are more significant than traditional rotors such as DCVJ.

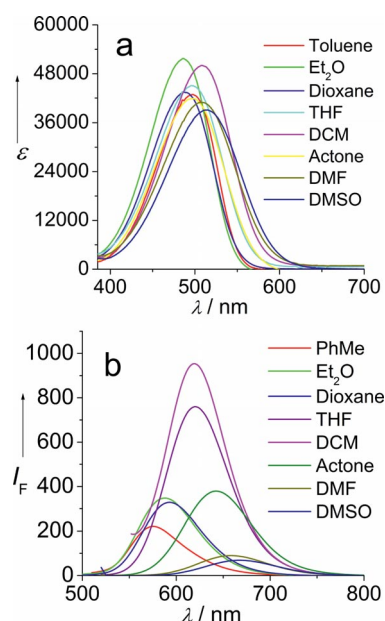


Figure 4. (a) UV/Vis absorption of rotor **4** in different solvents ($c = 1.0 \times 10^{-5}$ mol/L, 20 °C). (b) Fluorescence emission spectra of rotor **4** in different solvents ($c = 1.0 \times 10^{-5}$ mol/L, 20 °C).

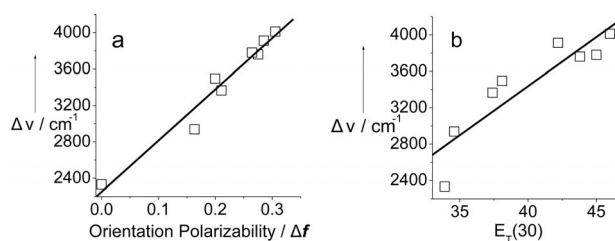


Figure 5. (a) Lippert–Mataga regressions and (b) plot of Stokes shifts vs. $E_T(30)$ values for rotor **4** in solvents ($c = 1.0 \times 10^{-5}$ mol/L, 20 °C).

Note that the sensitivity of the rotors to polarity is not a disadvantage; previously, it has been demonstrated that these kinds of viscosity molecular sensors can be used as dual-responsive molecular sensors of viscosity and polarity.^[2]

Our approach can be extended to other electron-donating chromophores [for example, phenothiazine (**6**; Scheme 1)], which shows absorption/emission wavelengths of 485/669 nm, respectively, and a Stokes shift of 184 nm (Figure 6). The emission intensity of rotor **6** is enhanced in viscous solvents (Figure 6); an x value of 0.609 was observed for rotor **6**.

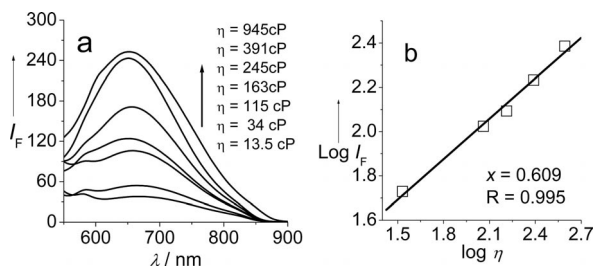


Figure 6. (a) Emission spectra of rotor **6** in mixtures of ethylene glycol/glycerol and (b) dependency of the emission intensity on the viscosity of the solvent ($\lambda_{\text{ex}} = 497$ nm, $\lambda_{\text{em}} = 652$ nm, $c = 1.0 \times 10^{-5}$ mol/L, 20 °C). The solid line in part (b) is the linear fitting according to the Förster–Hoffmann equation.

For a control rotor with phenyl but not the thiophene linker (**7**), the emission is poor (see the Supporting Information). Thus, thiophene insertion is crucial to improve the emission properties.

We noted that some new molecular rotors have been reported, such as those based on BODIPY. However, these BODIPY-based rotors give emission at 510 nm, and the Stokes shift is small (typical small Stokes shift of BODIPY fluorophores).^[13] In comparison, our new rotors give emissions at 600–700 nm, and the Stokes shifts are in the range of 100–200 nm.

Application of the Rotors to the Monitoring of the Phase Transition of Liquid Crystals by Fluorescence Intensity

The phase transition of liquid crystals is accompanied by significant viscosity variation. Thus, we used the new rotors to monitor the phase transition of a liquid crystal by fluorescence emission, because the emission of the rotors will be enhanced by the increase of the viscosity.

First, the molecular rotors were dissolved in the liquid crystal, and the mixture was heated to 80 °C, well beyond the clearing point of the liquid crystal (68 °C). With a decrease in the temperature, we observed a sharp increase in the emission intensity (Figure 7a), which is believed to be due to the transition from the liquid phase to the liquid crystal phase. A solution of rotor **3** in DMF was used as a control experiment. No enhanced emission was observed in the DMF solution upon lowering the temperature; thus, the enhancement of the emission of the rotor is due to the in-

crease in the viscosity of the liquid crystal and not to the reduced temperature. A similar result was found for rotor **6** (Figure 7b).

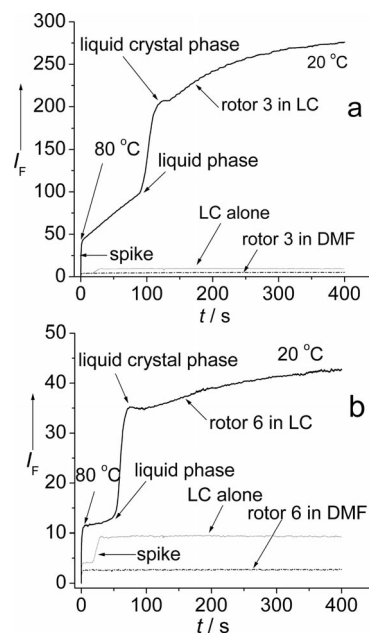


Figure 7. Use of molecular rotors to monitor the phase transitions of liquid crystal DYLC 7077-050 (LC) by monitoring the changes in fluorescence intensity vs. time (decreasing temperature of the liquid crystal). (a) Rotor **3** was dissolved in the liquid crystal ($\lambda_{\text{ex}} = 510$ nm, $\lambda_{\text{em}} = 658$ nm, $c = 3.0 \times 10^{-6}$ mol/L). A control experiment was carried out in DMF. (b) Use of the viscosity probe **6** to monitor the phase transitions of liquid crystal 761 (LC) by observing the changes in the fluorescence signal intensity vs. time. The probe **6** was dissolved in the liquid crystal ($\lambda_{\text{ex}} = 375$ nm, $\lambda_{\text{em}} = 389$ nm). For the control experiment, DMF was used ($\lambda_{\text{ex}} = 485$ nm, $\lambda_{\text{em}} = 778$ nm, $c = 3.0 \times 10^{-6}$ mol/L).

Density Functional Theory (DFT) Calculations

DFT calculations have recently been used to study the photophysical properties of fluorescent dyes,^[29] molecular probes,^[18–20,30–34] and luminescent materials.^[35–39] In this work we used DFT calculations to study the absorption and emission properties of the new molecular rotors to investigate the role of the thiophene moiety in the π conjugation of the molecular framework.

First, the ground-state geometry of the known rotor **2** was optimized. The molecule adopts a coplanar geometry. The UV/Vis absorptions of the rotors were calculated on the basis of the optimized ground-state geometry, and the results are presented in Table 2. The calculated absorption of 403 nm is close to the experimental value of 454 nm. The absorption maxima of other rotors were also calculated, and the results are close to the experimental values. For example, the absorption of rotors **3** and **4** were predicted to be 521 and 558 nm, respectively. These values are close to the experimental observations of 498 and 540 nm, respectively (Table 4). Thus, we can see that DFT calculations can be used to predict the absorptions of the rotors. The red-

Table 2. Selected parameters of the vertical excitation (UV/Vis absorptions) of compounds **1–4**. Electronic excitation energies, oscillator strengths (f), and configurations of the low-lying excited states of the probes and its fluorescent precursors calculated at the TDDFT//B3LYP/6-31G(d) level of theory based on the optimized ground-state geometry (the solvent methanol was considered in all the calculations).

Compound	Electronic transition ^[a]	TDDFT//B3LYP/6-31G(d)			
		Excitation energy ^[b] [eV]	f ^[c]	Composition ^[d]	CI ^[e]
1	$S_0 \rightarrow S_1$	3.18 (390)	1.0080	H \rightarrow L	0.7081
	$S_0 \rightarrow S_2$	4.24 (292)	0.0041	H - 2 \rightarrow L	0.1175
				H - 1 \rightarrow L	0.6381
				H \rightarrow L + 1	0.2747
2	$S_0 \rightarrow S_1$	3.08 (403)	1.0166	H \rightarrow L	0.7085
	$S_0 \rightarrow S_2$	3.97 (312)	0.0102	H - 1 \rightarrow L	0.6787
				H \rightarrow L + 1	0.1883
				H - 1 \rightarrow L	0.7495
3	$S_0 \rightarrow S_1$	2.38 (521)	1.0841	H \rightarrow L	0.7495
	$S_0 \rightarrow S_2$	3.56 (348)	0.2282	H - 1 \rightarrow L	0.2154
				H \rightarrow L + 1	0.2154
				H \rightarrow L	0.7108
4	$S_0 \rightarrow S_1$	2.22 (558)	1.2029	H \rightarrow L	0.1802
	$S_0 \rightarrow S_2$	3.47 (358)	0.3172	H - 2 \rightarrow L	0.6296
				H - 1 \rightarrow L	0.6296
				H \rightarrow L + 1	0.2610

[a] Only selected excited states were considered. [b] The numbers in parentheses are the excitation energies in wavelength [nm]. [c] Oscillator strength. [d] H represents the HOMO, and L represents the LUMO. Only the main configurations are presented. [e] Coefficient of the wavefunction for each excitation. The CI coefficients are absolute values.

Table 3. Emission-related electronic excitation energies, oscillator strengths (f), configurations of the low-lying excited states of the rotors **1–4** calculated at the TDDFT//B3LYP/6-31G(d) level of theory based on the optimized excited-state geometries (the solvent methanol was considered in all the calculations).

Compound	Electronic transition ^[a]	TDDFT//B3LYP/6-31G(d)			
		Excitation energy ^[b]	f ^[c]	Composition ^[d]	CI ^[e]
1	$S_0 \rightarrow S_1$	2.82 (439)	1.1592	H \rightarrow L	0.7076
	$S_0 \rightarrow S_2$	4.10 (302)	0.0109	H - 2 \rightarrow L	0.6710
				H \rightarrow L + 1	0.2071
2	$S_0 \rightarrow S_1$	2.73 (454)	1.1750	H \rightarrow L	0.7077
	$S_0 \rightarrow S_2$	3.80 (326)	0.0177	H - 1 \rightarrow L	0.6926
				H \rightarrow L + 1	0.1324
3	$S_0 \rightarrow S_1$	2.10 (589)	1.3053	H \rightarrow L	0.7076
	$S_0 \rightarrow S_2$	3.39 (366)	0.1986	H - 1 \rightarrow L	0.6860
				H \rightarrow L + 1	0.1460
4	$S_0 \rightarrow S_1$	1.98 (628)	1.3873	H \rightarrow L	0.7085
	$S_0 \rightarrow S_2$	3.39 (366)	0.2792	H - 1 \rightarrow L	0.6735
				H \rightarrow L + 1	0.1991

[a] Only selected excited states were considered. [b] The numbers in parentheses are the excitation energies in wavelength [nm]. [c] Oscillator strength. [d] H represents the HOMO, and L represents the LUMO. Only the main configurations are presented. [e] Coefficient of the wavefunction for each excitation. The CI coefficients are absolute values.

shifted absorptions and emissions of the new rotors can be attributed to the extended π -conjugation frameworks of the rotors due to the π -conjugation linker of the thiophene moiety. For example, the frontier molecular orbitals of rotor **4** are distributed over the whole molecular framework (see Figure 9).

The calculated excitation energies of the rotors are summarized in Table 2. To study the fluorescence emission of the rotors, the singlet excited states of the rotors were optimized, and the emission wavelengths were calculated by the TDDFT method based on the optimized S_1 excited-state geometries (Table 3).

The calculated emission wavelengths of the probes are close to the experimental values (Table 4). For example, the calculated emission wavelength for rotor **2** is 454 nm, which is close to the experimental value of 499 nm. For rotor **3**,

the calculated emission wavelength is 589 nm, which is close to the experimental value of 647 nm. The calculated Stokes shifts are in line with the experimental results.

Table 4. Theoretical values calculated at the TDDFT//B3LYP/6-31G(d) level of theory and measured values of the absorption and emission wavelengths (the solvent methanol was considered in all the calculations).

Compound	Theoretical value		Measured value	
	λ_{ab} ^[a] [nm]	λ_{em} ^[b] [nm]	λ_{ab} [nm]	λ_{em} [nm]
1	390	439	438	480
2	403	454	454	499
3	521	589	498	647
4	558	628	540	681

[a] Maximum UV/Vis absorption wavelength. [b] Maximum fluorescence emission wavelength.

The frontier molecular orbitals involved in the singlet excited states of the rotors are presented in Figures 8 and 9 (for other rotors, see the Supporting Information). From these MOs, it is clear that their energy levels are different to those at the ground-state geometries. This discrepancy is reasonable, because the conformation relaxation will follow the Frank–Condon excitation. The DFT calculations on the

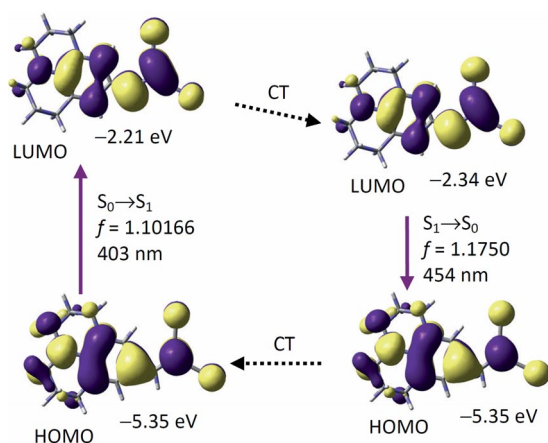


Figure 8. Frontier molecular orbitals (MOs) of rotor **2** involved in the vertical excitation (i.e., UV/Vis absorption, left column) and emission (right column). For the DFT calculations methanol was employed as the solvent. The vertical excitation calculations are based on the optimized ground-state geometry (S_0 state) and the emission calculations are based on the optimized excited state (S_1 state) performed at the B3LYP/6-31G(d) level of theory by using Gaussian 09W. CT represents the conformation transformation. Excitation and radiative processes are marked as solid lines, and non-radiative processes are marked by dotted lines.

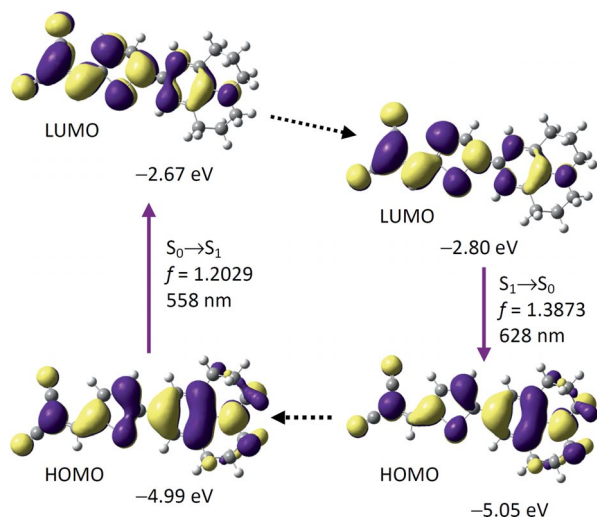


Figure 9. Frontier molecular orbitals (MOs) of rotor **4** involved in the vertical excitation (i.e., UV/Vis absorption, left column) and emission (right column). For the DFT calculations methanol was employed as the solvent. The vertical excitation calculations are based on the optimized ground-state geometry (S_0 state) and the emission calculations are based on the optimized excited state (S_1 state) performed at the B3LYP/6-31G(d) level of theory by using Gaussian 09W. CT represents the conformation transformation. Excitation and radiative processes are marked as solid lines, and the non-radiative processes are marked by dotted lines.

ground and S_1 excited states of the rotors show that for the traditional rotors, the ground-to-excited-state transition electric dipole moments (ca. 2 D) are much smaller than those of the thiophene rotors (ca. 10 D). Larger dipole moment changes in the S_1 state than in the S_0 state will induce larger Stokes shifts.^[40]

Conclusions

Thiophene-inserted aryl–dicyanovinyl molecular rotors have been prepared, and the absorption/emission wavelengths and Stokes shifts were substantially improved compared with those of the traditional molecules [for example, rotor **4** shows absorption/emission wavelengths of 559/697 nm, respectively, and a very large Stokes shift of 138 nm]. For the conventional molecular rotor **2**, these photophysical parameters are 465/503 nm and 38 nm, respectively. We also demonstrated that the strategy of the thiophene-linked donor–acceptor can be used to prepare more functionalized rotors and can be extended to other fluorophores such as phenothiazine. The role of π conjugation of the thiophene moiety was proved by DFT calculations, which successfully predicted the UV/Vis absorption and fluorescence emission wavelengths. The molecular rotors can be used to monitor the phase transition of liquid crystals by monitoring the fluorescence intensity enhancement upon decreasing the temperature of the liquid crystal. We believe these results will inspire the design of new fluorescent rotors for molecular viscosity sensing.

Experimental Section

General Methods and Analytical Measurements: NMR spectra were recorded with a 400 MHz Varian Unity Inova spectrometer. Mass spectra were recorded with a Q-TOF Micro MS spectrometer. UV/Vis spectra were recorded with an HP8453 UV/Vis spectrophotometer. Fluorescence spectra were recorded with JASCO FP-6500 and Sanco 970 CRT spectrofluorimeters. Fluorescence quantum yields were measured with quinine sulfate as reference ($\Phi = 0.547$ in 0.05 M H_2SO_4). Fluorescence lifetimes were measured with a Horiba Jobin Yvon Fluoro Max-4 (TCSPC) instrument. *p*-Iodo-*N,N*-dimethylaniline (**3a**),^[41] methyl 6-iodo-3,4-dihydro-1(2*H*)-quinoline-1-propionate (**5a**),^[41] *N*-[2-(methoxycarbonyl)ethyl]-1,2,3,4-tetrahydroquinoline (precursor of compound **5a**),^[42] 2-formyl-5-[4'-(dimethylamino)phenyl]thiophene (**3b**), julolidine (**4a**),^[43] and 4-bromojulolidine (**4b**)^[44] were synthesized according to literature procedures. The liquid crystal used in the viscosity sensing was DYLC 7077-050 (nematic-phase liquid crystal, clearing point 68 °C).

5-[4-(Dimethylamino)phenyl]thiophene-2-carbaldehyde (3b): 5-Formylthiophene-2-boronic acid (187 mg, 1.2 mmol) and *p*-iodo-*N,N*-dimethylaniline (247.0 mg, 1.0 mmol) were dissolved in a mixture of toluene (5.0 mL), aqueous K_2CO_3 (1.0 mL, 2 M) and ethanol (5 mL) under argon, and then $[Pd(PPh_3)_4]$ (58.0 mg, 0.05 mmol) was added. The mixture was stirred at 85 °C for 3 h. After removal of the solvent under reduced pressure, water was added to the mixture, and the product was extracted with dichloromethane. The organic layer was collected and dried with anhydrous Na_2SO_4 . Then the residue was purified by column chromatography (silica gel;

dichloromethane) to give the product as a yellow solid. Yield: 182.0 mg, 79.0%. $^1\text{H NMR}$ (400 MHz, CDCl_3): δ = 9.82 (s, 1 H, CHO), 7.67 (d, J = 4.0 Hz, 1 H, thiophene-CH), 7.55 (d, J = 8.0 Hz, 2 H, Ar-CH), 7.24 (d, J = 4.0 Hz, 1 H, thiophene-CH), 6.70 (d, J = 8.0 Hz, 2 H, Ar-CH), 3.02 (s, 6 H, CH_3) ppm. MS (TOF EI): calcd. for $[\text{C}_{13}\text{H}_{13}\text{NOS} + \text{H}]^+$ 231.0718; found 231.0723.

({5-[4-(Dimethylamino)phenyl]thiophen-2-yl}methylidene)propanedinitrile (3): Compound **3b** (69.0 mg, 0.30 mmol) and malononitrile (60.0 mg, 0.36 mmol) were dissolved in CH_2Cl_2 (5 mL), and Al_2O_3 (92.0 mg, 0.9 mmol) was added as catalyst and desiccator. The mixture was stirred at 20 °C for 1 h. The solvent was evaporated under reduced pressure, and the crude product was purified by column chromatography (silica gel; $\text{CH}_2\text{Cl}_2/\text{CH}_3\text{OH}$ = 50:1, v/v) to give a red solid. Yield: 63.0 mg, 75.2%. $^1\text{H NMR}$ (400 MHz, CDCl_3): δ = 7.69 (s, 1 H, CH=CH), 7.60 (d, J = 4.0 Hz, 1 H, thiophene-CH), 7.57 (d, J = 12.0 Hz, 2 H, Ar-CH), 7.27 (d, J = 4.0 Hz, 1 H, thiophene-CH), 6.69 (d, J = 12.0 Hz, 2 H, Ar-CH), 3.06 (s, 6 H, CH_3) ppm. $^{13}\text{C NMR}$ (100 MHz, CDCl_3): δ = 159.1, 151.8, 150.3, 141.1, 132.1, 128.1, 122.1, 120.0, 115.2, 114.3, 112.2, 73.4, 40.3 ppm. MS (TOF EI): calcd. for $[\text{C}_{16}\text{H}_{13}\text{N}_3\text{S} + \text{H}]^+$ 279.0830; found 279.0836.

5-(2,3,6,7-Tetrahydro-1*H*,5*H*-pyrido[3,2,1-*ij*]quinolin-9-yl)thiophene-2-carbaldehyde (4c): The reaction was carried out according to the procedure used for the preparation of **3b**. The crude product was purified by column chromatography (silica gel; CH_2Cl_2) to give the product as a yellow solid. Yield: 60.0 mg, 42.4%. $^1\text{H NMR}$ (400 MHz, CDCl_3): δ = 9.78 (s, 1 H, CHO), 7.63 (d, J = 4.0 Hz, 1 H, thiophene-CH), 7.16 (d, J = 4.0 Hz, 1 H, thiophene-CH), 7.11 (s, 2 H, Ar-CH), 3.21 (t, J = 12.0 Hz, 4 H, CH_2), 2.76 (t, J = 12.0 Hz, 4 H, CH_2), 1.94–2.00 (m, 4 H, CH_2) ppm. MS (TOF EI): calcd. for $[\text{C}_{17}\text{H}_{17}\text{NOS} + \text{H}]^+$ 283.1031; found 283.1035.

{5-(2,3,6,7-Tetrahydro-1*H*,5*H*-pyrido[3,2,1-*ij*]quinolin-9-yl)thiophen-2-yl}methylidene}propanedinitrile (4): The reaction was carried out according to the procedure used for the synthesis of **3**. The crude product was purified by column chromatography (silica gel; CH_2Cl_2) to give a red solid. Yield: 36.0 mg, 85.3%. $^1\text{H NMR}$ (400 MHz, CDCl_3): δ = 7.62 (s, 1 H, CH=CH), 7.53 (d, J = 4.0 Hz, 1 H, thiophene-CH), 7.18 (d, J = 4.0 Hz, 1 H, thiophene-CH), 7.14 (s, 2 H, Ar-CH), 3.26 (t, J = 8.0 Hz, 4 H, CH_2), 2.76 (t, J = 12.0 Hz, 4 H, CH_2), 1.94–2.00 (m, 4 H, CH_2) ppm. $^{13}\text{C NMR}$ (100 MHz, CDCl_3): δ = 160.0, 149.9, 145.2, 141.4, 131.5, 125.7, 121.5, 121.4, 118.7, 115.5, 114.6, 71.8, 50.0, 27.8, 21.6 ppm. MS (TOF EI): calcd. for $[\text{C}_{20}\text{H}_{17}\text{N}_3\text{S} + \text{H}]^+$ 331.1143; found 331.1153.

Ethyl 3-[6-(5-Formylthiophen-2-yl)-3,4-dihydroquinolin-1(2*H*)-yl]propanoate (5b): The reaction was carried out according to the procedure used for the synthesis of **3b**. The crude product was purified by column chromatography (silica gel; CH_2Cl_2) to give a yellow solid. Yield: 85.0 mg, 78.2%. $^1\text{H NMR}$ (400 MHz, CDCl_3): δ = 9.80 (s, 1 H, CHO), 7.65 (d, J = 4.0 Hz, 1 H, thiophene-CH), 7.39 (d, J = 4.0 Hz, 1 H, Ar-CH), 7.37 (s, 1 H, Ar-CH), 7.19 (d, J = 4.0 Hz, 1 H, thiophene-CH), 6.58 (d, J = 8.0 Hz, 1 H, Ar-CH), 4.14 (t, J = 12.0 Hz, 2 H, CH_2), 3.65 (t, J = 16.0 Hz, 2 H, CH_2), 3.35 (t, J = 12.0 Hz, 2 H, CH_2), 2.77 (t, J = 12.0 Hz, 2 H, CH_2), 2.60 (t, J = 12.0 Hz, 2 H, CH_2), 1.95–1.99 (m, 2 H, CH_2), 1.26 (t, J = 16.0 Hz, 3 H, CH_3) ppm. $^{13}\text{C NMR}$ (100 MHz, CDCl_3): δ = 182.5, 172.2, 156.2, 145.9, 140.0, 138.3, 127.4, 125.8, 123.0, 121.4, 120.7, 110.5, 60.9, 49.6, 47.1, 31.6, 28.1, 21.9, 14.3 ppm. It should be noted that ethanol was used as solvent for the reaction; we found that the methyl ester was transformed into the ethyl ester.

Ethyl 3-[6-[5-(2,2-Dicyanoethenyl)thiophen-2-yl]-3,4-dihydroquinolin-1(2*H*)-yl]propanoate (5): The reaction was carried out according to the procedure used for the synthesis of **3**. The crude product was purified by column chromatography (silica gel;

CH_2Cl_2) to give a red solid. Yield: 41.0 mg, 89.2%. $^1\text{H NMR}$ (400 MHz, CDCl_3): δ = 7.62 (s, 1 H, CH=CH), 7.54 (d, J = 4.0 Hz, 1 H, thiophene-CH), 7.39 (d, J = 12.0 Hz, 1 H, Ar-CH), 7.25 (s, 1 H, Ar-CH), 7.18 (d, J = 4.0 Hz, 1 H, thiophene-CH), 6.54 (d, J = 8.0 Hz, 1 H, Ar-CH), 4.09 (t, J = 12.0 Hz, 2 H, CH_2), 3.63 (t, J = 12.0 Hz, 2 H, CH_2), 3.34 (t, J = 12.0 Hz, 2 H, CH_2), 2.73 (t, J = 12.0 Hz, 2 H, CH_2), 2.57 (t, J = 12.0 Hz, 2 H, CH_2), 1.91–1.94 (m, 2 H, CH_2), 1.22 (t, J = 12.0 Hz, 3 H, CH_3) ppm. $^{13}\text{C NMR}$ (100 MHz, CDCl_3): δ = 172.0, 159.2, 150.1, 146.8, 141.2, 131.9, 127.8, 126.3, 123.2, 121.8, 119.8, 115.2, 114.3, 110.5, 72.8, 60.9, 49.7, 47.1, 31.7, 28.0, 21.8, 14.3 ppm. HRMS (ESI): calcd. for $[\text{C}_{22}\text{H}_{21}\text{N}_3\text{O}_2\text{S} + \text{Na}]^+$ 414.1252; found 414.1253.

10-Butyl-10*H*-phenothiazine (6a): *n*- $\text{C}_4\text{H}_9\text{Br}$ (1.64 g, 12 mmol) was added to a stirred solution of phenothiazine (1.99 g, 10 mmol), hexadecyltrimethylammonium bromide (CTAB) (0.1 g), and NaOH (0.6 g) in acetone (10 mL). The mixture was heated at reflux for 6 h. Then the solvent was removed. The residue was extracted with dichloromethane (DCM) and washed with water. The organic phase was dried with anhydrous Na_2SO_4 . The solvent was removed, and the residue was purified by column chromatography (silica gel; DCM/petroleum ether = 1:3, v/v) to give the product as a light-green liquid. Yield: 1.2 g, 47.0%. $^1\text{H NMR}$ (CDCl_3 , 400 MHz): δ = 7.10–7.14 (m, 4 H, Ar-CH), 6.86 (t, J = 8.0 Hz, 2 H, Ar-CH), 6.83 (d, J = 8.0 Hz, 2 H, Ar-CH), 3.81 (t, J = 12.0 Hz, 2 H, CH_2), 1.72–1.80 (m, 2 H, CH_2), 1.40–1.46 (m, 2 H, CH_2), 0.92 (t, J = 12.0 Hz, 3 H, CH_3) ppm.

3-Bromo-10-butyl-10*H*-phenothiazine (6b): A solution of NaOH (0.165 g, 1.61 mmol) in glacial acetic acid (10 mL) was added to a solution of **6a** (0.35 g, 1.37 mmol) in chloroform (5 mL) followed by dropwise addition of a solution of bromine (0.07 mL, 1.37 mmol) in glacial acetic acid (3 mL) at 0 °C. The mixture was stirred at 0–5 °C for 2 h. The solvents were removed, and, after addition of water (15 mL) and dichloromethane (25 mL), the organic layer was separated and dried with Na_2SO_4 . The solvent was removed, and the residue was purified by column chromatography (silica gel; DCM/petroleum ether, 1:3, v/v) to give the product as a light-yellow liquid. Yield: 0.31 g, 67.8%. $^1\text{H NMR}$ (CDCl_3 , 400 MHz): δ = 7.17 (d, J = 8.0 Hz, 2 H, Ar-CH), 7.06–7.13 (m, 2 H, Ar-CH), 6.86 (t, J = 8.0 Hz, 1 H, Ar-CH), 6.80 (d, J = 8.0 Hz, 1 H, Ar-CH), 6.60 (t, J = 8.0 Hz, 1 H, Ar-CH), 3.75 (t, J = 12.0 Hz, 2 H, CH_2), 1.68–1.75 (m, 2 H, CH_2), 1.35–1.43 (m, 2 H, CH_2), 0.90 (t, J = 12.0 Hz, 3 H, CH_3) ppm. MS (APCI): calcd. for $[\text{C}_{16}\text{H}_{16}\text{BrNS} + \text{H}]^+$ 335.3; found 335.1.

5-(10-Butyl-10*H*-phenothiazin-3-yl)thiophene-2-carbaldehyde (6c): Compound **6b** (668.5 mg, 2.0 mmol), 2.0 M aqueous K_2CO_3 solution (10 mL), and $[\text{Pd}(\text{PPh}_3)_4]$ (115 mg, 0.1 mmol) in THF (15 mL) were heated to 50 °C and stirred under argon for 0.5 h. 5-Formylthienyl-2-boronic acid (376 mg, 2.4 mmol) in THF (15 mL) was added, and the mixture was heated at reflux for 24 h. After completion of the reaction, water (15 mL) was added, and the product was extracted with DCM. The organic layer was collected and dried with anhydrous Na_2SO_4 . Then the residue was purified by column chromatography (silica gel; DCM/petroleum ether, 1:1, v/v) to give the product as a yellow solid. Yield: 211.0 mg, 28.9%. $^1\text{H NMR}$ (CDCl_3 , 400 MHz): δ = 9.81 (s, 1 H, CHO), 7.63 (d, J = 4.0 Hz, 1 H, thiophene-CH), 7.37 (d, J = 8.0 Hz, 1 H, Ar-CH), 7.34 (s, 1 H, Ar-CH), 7.21 (d, J = 4.0 Hz, 1 H, thiophene-CH), 7.09–7.16 (m, 2 H, Ar-CH), 6.92 (t, J = 16.0 Hz, 1 H, Ar-CH), 6.84 (d, J = 16.0 Hz, 1 H, Ar-CH), 6.79 (t, J = 8.0 Hz, 1 H, Ar-CH), 3.82 (t, J = 16.0 Hz, 2 H, CH_2), 1.73–1.80 (m, 2 H, CH_2), 1.41–1.47 (m, 2 H, CH_2), 0.93 (t, J = 16.0 Hz, 3 H, CH_3) ppm. MS (TOF EI): calcd. for $[\text{C}_{21}\text{H}_{19}\text{NOS}_2 + \text{H}]^+$ 365.0908; found 365.0918.

{[5-(10-Butyl-10H-phenothiazin-3-yl)thiophen-2-yl]methylidene}propanedinitrile (6): The reaction was carried out according to the procedure used for the synthesis of **3**. The crude product was purified by column chromatography (silica gel; DCM/petroleum ether, 2:1, v/v) to give a red solid. Yield: 37.0 mg, 87.3%. ¹H NMR (CDCl₃, 400 MHz): δ = 7.67 (s, 1 H, Ar-CH), 7.59 (d, *J* = 4.0 Hz, 1 H, Ar-CH), 7.41 (t, *J* = 8.0 Hz, 1 H, Ar-CH), 7.34 (s, 1 H, CH₂=CH₂), 7.22 (d, *J* = 4.0 Hz, 1 H, thiophene-CH), 7.08–7.16 (m, 2 H, Ar-CH), 6.92 (d, *J* = 16.0 Hz, 1 H, Ar-CH), 6.84 (d, *J* = 8.0 Hz, 1 H, thiophene-CH), 6.79 (d, *J* = 12.0 Hz, 1 H, Ar-CH), 3.83 (t, *J* = 16.0 Hz, 2 H, CH₂), 1.72–1.80 (m, 2 H, CH₂), 1.41–1.48 (m, 2 H, CH₂), 0.92 (t, *J* = 16.0 Hz, 3 H, CH₃) ppm. ¹³C NMR (100 MHz, CDCl₃): δ = 156.1, 150.4, 147.3, 144.2, 140.4, 133.5, 127.8, 127.7, 126.5, 126.1, 126.0, 125.2, 123.8, 123.6, 123.3, 117.0, 115.9, 115.6, 114.6, 113.7, 47.6, 29.1, 20.3, 13.9 ppm. MS (TOF EI): calcd. for [C₂₄H₁₉N₃S₂ + H]⁺ 413.1020; found 413.1031.

4-(2,3,6,7-Tetrahydro-1H,5H-pyrido[3,2,1-ij]quinolin-9-yl)benzaldehyde (7a): The reaction was carried out according to the procedure used for the synthesis of **3b**. The crude product was purified by column chromatography (silica gel; DCM/petroleum ether, 3:1, v/v) to give a yellow solid. Yield: 69.0 mg, 86.3%. ¹H NMR (400 MHz, CDCl₃): δ = 9.98 (s, 1 H, CHO), 7.84 (d, *J* = 8.0 Hz, 2 H, Ar-CH), 7.66 (d, *J* = 8.0 Hz, 2 H, Ar-CH), 7.13 (s, 2 H, Ar-CH), 3.21 (t, *J* = 12.0 Hz, 4 H, CH₂), 2.82 (t, *J* = 16.0 Hz, 4 H, CH₂), 1.97–2.03 (m, 4 H, CH₂) ppm. MS (TOF EI): calcd. for [C₁₉H₁₉NO + H]⁺ 277.1467; found 277.1468.

[4-(2,3,6,7-Tetrahydro-1H,5H-pyrido[3,2,1-ij]quinolin-9-yl)benzylidene]propanedinitrile (7): The reaction was carried out according to the procedure used for the synthesis of **3**. The crude product was purified by column chromatography (silica gel; DCM) to give a red solid. Yield: 42 mg, 89.5%. ¹H NMR (400 MHz, CDCl₃): δ = 7.86 (d, *J* = 8.0 Hz, 2 H, Ar-CH), 7.66 (s, 1 H, CH=CH), 7.64 (d, *J* = 4.0 Hz, 2 H, Ar-CH), 7.15 (s, 2 H, Ar-CH), 3.24 (t, *J* = 12.0 Hz, 4 H, CH₂), 2.81 (t, *J* = 12.0 Hz, 4 H, CH₂), 1.97–2.02 (m, 4 H, CH₂) ppm. ¹³C NMR (100 MHz, CDCl₃): δ = 159.2, 147.9, 144.1, 131.8, 128.1, 126.0, 125.9, 124.7, 121.8, 114.8, 113.6, 79.1, 50.0, 28.0, 21.9 ppm. MS (TOF EI): calcd. for [C₂₂H₁₉N₃ + H]⁺ 325.1579; found 325.1589.

DFT Calculations: [45] All the calculations were based on density functional theory (DFT) with B3LYP functional and 6-31G(d) basis set. Solvent methanol was considered in all the calculations (CPCM model). The UV/Vis absorption of the compounds (vertical excitation) were calculated with the TDDFT methods based on the optimized ground state geometry (S₀ state). For the fluorescence emission, the emission wavelength were calculated based on the optimized excited states (in most cases S₁ state). All these calculations were performed with Gaussian 09W.

Supporting Information (see footnote on the first page of this article): More synthesis details, structural characterization data, and photophysical properties of the rotors.

Acknowledgments

We thank the National Natural Science Foundation of China (NSFC) (20972024 and 21073028), the Fundamental Research Funds for the Central Universities (DUT10ZD212 and DUT11LK19), the Royal Society (UK) and NSFC China-UK Cost-Share Science Networks (21011130154), the Ministry of Education (SRFDP-200801410004 and NCET-08-0077), the Education Department of Liaoning Province (2009 T015) and the State Key Laboratory of Fine Chemicals (KF0802) for financial support.

- [1] M. A. Haidekker, E. A. Theodorakis, *Org. Biomol. Chem.* **2007**, *5*, 1669–1678.
- [2] A. Jacobson, A. Petric, D. Hogenkamp, A. Sinur, J. R. Barrio, *J. Am. Chem. Soc.* **1996**, *118*, 5572–5579.
- [3] M. A. Haidekker, T. P. Brady, D. Lichlyter, E. A. Theodorakis, *J. Am. Chem. Soc.* **2006**, *128*, 398–399.
- [4] D. Allen, A. C. Benniston, A. Harriman, S. A. Rostron, C. Yu, *Phys. Chem. Chem. Phys.* **2005**, *7*, 3035–3040.
- [5] L. L. Zhu, X. Li, F. Y. Ji, X. Ma, Q. C. Wang, H. Tian, *Langmuir* **2009**, *25*, 3482–3486.
- [6] M. A. Haidekker, T. P. Brady, S. H. Chalian, W. Akers, D. Lichlyter, E. A. Theodorakis, *Bioorg. Chem.* **2004**, *32*, 274–289.
- [7] A. Paul, A. Samanta, *J. Phys. Chem. B* **2008**, *112*, 16626–16632.
- [8] M. A. Haidekker, T. T. Ling, M. Anglo, H. Y. Stevens, J. A. Frangos, E. A. Theodorakis, *Chem. Biol.* **2001**, *8*, 123–131.
- [9] M. Lindgren, K. Sörgjerd, P. Hammarström, *Biophys. J.* **2005**, *88*, 4200–4212.
- [10] B. Mennucci, C. Cappelli, C. A. Guido, R. Cammi, J. Tomasi, *J. Phys. Chem. A* **2009**, *113*, 3009–3020.
- [11] J. R. Lakowicz, *Principles of Fluorescence Spectroscopy*, 2nd ed., Kluwer Academic, New York, **1999**.
- [12] K. P. Ghigginio, J. A. Hutchison, S. J. Langford, M. J. Latter, M. A. P. Lee, P. R. Lowenstern, C. Scholes, M. Takezaki, B. E. Wilman, *Adv. Funct. Mater.* **2007**, *17*, 805–813.
- [13] a) M. K. Kuimova, G. Yahiogly, J. A. Levitt, K. Suhling, *J. Am. Chem. Soc.* **2008**, *130*, 6672–6673; b) J. A. Levitt, M. K. Kuimova, G. Yahiogly, P. H. Chung, K. Suhling, D. Phillips, *J. Phys. Chem. C* **2009**, *113*, 11634–11642.
- [14] J. Cody, S. Mandal, L. Yang, C. J. Fahrni, *J. Am. Chem. Soc.* **2008**, *130*, 13023–13032.
- [15] D. Zhu, M. A. Haidekker, J. S. Lee, Y. Y. Won, J. C. M. Lee, *Macromolecules* **2007**, *40*, 7730–7732.
- [16] M. K. Kuimova, S. W. Botchway, A. W. Parker, M. Balaz, H. A. Collins, H. L. Anderson, K. Suhling, P. R. Ogilby, *Nat. Chem.* **2009**, *1*, 69–73.
- [17] X. Peng, Z. Yang, J. Wang, J. Fan, Y. He, F. Song, B. Wang, S. Sun, J. Qu, J. Qi, M. Yan, *J. Am. Chem. Soc.* **2011**, *133*, 6626–6635.
- [18] X. Zhang, L. Chi, S. Ji, Y. Wu, P. Song, K. Han, H. Guo, T. D. James, J. Zhao, *J. Am. Chem. Soc.* **2009**, *131*, 17452–17463.
- [19] S. Ji, J. Yang, Q. Yang, S. Liu, M. Chen, J. Zhao, *J. Org. Chem.* **2009**, *74*, 4855–4865.
- [20] S. Ji, H. Guo, X. Yuan, X. Li, H. Ding, P. Gao, C. Zhao, W. Wu, W. Wu, J. Zhao, *Org. Lett.* **2010**, *12*, 2876–2879.
- [21] F. Zhou, J. Shao, Y. Yang, J. Zhao, H. Guo, X. Li, S. Ji, Z. Zhang, *Eur. J. Org. Chem.* **2011**; DOI: 10.1002/ejoc.201100606.
- [22] Q. Zheng, B. J. Jung, J. Sun, H. E. Katz, *J. Am. Chem. Soc.* **2010**, *132*, 5394–5404.
- [23] F. Silvestri, A. Marrocchi, M. Seri, C. Kim, T. J. Marks, A. Facchetti, A. Taticchi, *J. Am. Chem. Soc.* **2010**, *132*, 6108–6123.
- [24] Y. Wu, H. Guo, T. D. James, J. Zhao, *J. Org. Chem.* **2011**, *76*, 5685–5695.
- [25] M. A. Haidekker, W. J. Alkers, *Opt. Lett.* **2006**, *31*, 2529–2531.
- [26] M. A. Haidekker, T. P. Brady, D. Lichlyter, E. A. Theodorakis, *Bioorg. Chem.* **2005**, *33*, 415–425.
- [27] Y. Wu, H. Guo, J. Shao, X. Zhang, S. Ji, J. Zhao, *J. Fluoresc.* **2011**, *21*, 1143–1154.
- [28] F. Han, L. Chi, W. Wu, X. Liang, M. Fu, J. Zhao, *J. Photochem. Photobiol. A: Chem.* **2008**, *196*, 10–23.
- [29] G. Zhao, J. Liu, L. Zhou, K. Han, *J. Phys. Chem. B* **2007**, *111*, 8940–8945.
- [30] X. Zhang, Y. Wu, S. Ji, H. Guo, P. Song, K. Han, W. Wu, W. Wu, T. D. James, J. Zhao, *J. Org. Chem.* **2010**, *75*, 2578–2588.
- [31] H. Guo, Y. Jing, X. Yuan, S. Ji, J. Zhao, X. Li, Y. Kan, *Org. Biomol. Chem.* **2011**, *9*, 3844–3853.
- [32] J. Shao, H. Guo, S. Ji, J. Zhao, *Biosens. Bioelectron.* **2011**, *26*, 3012–3017.

- [33] T. Kowalczyk, Z. Lin, T. V. Voorhis, *J. Phys. Chem. A* **2010**, *114*, 10427–10434.
- [34] J. D. Larkin, J. S. Fossey, T. D. James, B. R. Brooks, C. W. Bock, *J. Phys. Chem. A* **2010**, *114*, 12531–12539.
- [35] G.-J. Zhou, Q. Wang, W.-Y. Wong, D. Ma, L. Wang, Z. Lin, *J. Mater. Chem.* **2009**, *19*, 1872–1883.
- [36] Z. He, W. Y. Wong, X. Xu, H. S. Kwok, Z. Lin, *Inorg. Chem.* **2006**, *45*, 10922–10937.
- [37] D. N. Kozhevnikov, V. N. Kozhevnikov, M. Z. Shafikov, A. M. Prokhorov, D. W. Bruce, J. A. G. Williams, *Inorg. Chem.* **2006**, *45*, 10922–10937.
- [38] K. Hanson, A. Tamayo, V. V. Diev, M. T. Whited, P. I. Djurovich, M. E. Thompson, *Inorg. Chem.* **2010**, *49*, 6077–6084.
- [39] P. Shao, Y. Li, A. Azenkeng, M. R. Hoffmann, W. Sun, *Inorg. Chem.* **2009**, *48*, 2407–2419.
- [40] J. R. Lakowicz, *Principles of Fluorescence Spectroscopy*, 2nd ed., Plenum Press, New York, **1999**.
- [41] J. J. L. Clar, *J. Am. Chem. Soc.* **1997**, *119*, 7676–7684.
- [42] S. I. Agbo, G. Hallas, A. D. Towns, *Dyes Pigm.* **2000**, *47*, 33–43.
- [43] D. B. Glass, A. Weissberger, *Org. Synth.* **1946**, *26*, 40.
- [44] E. Z. Colman, J. S. Siegel, *Can. J. Chem.* **2009**, *87*, 440–447.
- [45] M. J. Frisch, G. W. Trucks, H. B. Schlegel, G. E. Scuseria, M. A. Robb, J. R. Cheeseman, G. Scalmani, V. Barone, B. Mennucci, G. A. Petersson, H. Nakatsuji, M. Caricato, X. Li, H. P. Hratchian, A. F. Izmaylov, J. Bloino, G. Zheng, J. L. Sonnenberg, M. Hada, M. Ehara, K. Toyota, R. Fukuda, J. Hasegawa, M. Ishida, T. Nakajima, Y. Honda, O. Kitao, H. Nakai, T. Vreven, J. A. Montgomery Jr., J. E. Peralta, F. Ogliaro, M. Bearpark, J. J. Heyd, E. Brothers, K. N. Kudin, V. N. Staroverov, R. Kobayashi, J. Normand, K. Raghavachari, A. Rendell, J. C. Burant, S. S. Iyengar, J. Tomasi, M. Cossi, N. Rega, J. M. Millam, M. Klene, J. E. Knox, J. B. Cross, V. Bakken, C. Adamo, J. Jaramillo, R. Gomperts, R. E. Stratmann, O. Yazyev, A. J. Austin, R. Cammi, C. Pomelli, J. W. Ochterski, R. L. Martin, K. Morokuma, V. G. Zakrzewski, G. A. Voth, P. Salvador, J. J. Dannenberg, S. Dapprich, A. D. Daniels, Ö. Farkas, J. B. Foresman, J. V. Ortiz, J. Cioslowski, D. J. Fox, *Gaussian 09W*, Revision A.1, Gaussian, Inc., Wallingford, CT, **2009**.

Received: June 18, 2011

Published Online: August 25, 2011